Journal of Molecular Graphics and Modelling 76 (2017) 77–85

Contents lists available at ScienceDirect

Journal of Molecular Graphics and Modelling

journal homepage: www.elsevier.com/locate/JMGM

Topical Perspectives

Investigation of the binding free energies of FDA approved drugs against subtype B and C-SA HIV PR: ONIOM approach

Z.K. Sanusi[a], T. Govender[a], G.E.M. Maguire[a,b], S.B. Maseko[a], J. Lin[c], H.G. Kruger[a,*], B. Honarparvar[a,*]

[a] Catalysis and Peptide Research Unit, School of Health Sciences, University of KwaZulu-Natal, Durban 4001, South Africa
[b] School of Chemistry and Physics, University of KwaZulu-Natal, 4001 Durban, South Africa
[c] School of Life Sciences, University of KwaZulu-Natal, Durban 4001, South Africa

ARTICLE INFO

Article history:
Received 1 April 2017
Received in revised form 8 June 2017
Accepted 9 June 2017
Available online 29 June 2017

Keywords:
HIV subtype B/C-SA PR
HIV PR inhibitors
Inhibitor—enzyme interactions
Our Own N-layered Integrated molecular Orbital and molecular Mechanics (ONIOM)
Binding free energies

ABSTRACT

Human immune virus subtype C is the most widely spread HIV subtype in Sub-Sahara Africa and South Africa. A profound structural insight on finding potential lead compounds is therefore necessary for drug discovery. The focus of this study is to rationalize the nine Food and Drugs Administration (FDA) HIV antiviral drugs complexed to subtype B and C-SA PR using ONIOM approach. To achieve this, an integrated two-layered ONIOM model was used to optimize the geometrics of the FDA approved HIV-1 PR inhibitors for subtype B. In our hybrid ONIOM model, the HIV-1 PR inhibitors as well as the ASP 25/25′ catalytic active residues were treated at high level quantum mechanics (QM) theory using B3LYP/6-31G(d), and the remaining HIV PR residues were considered using the AMBER force field. The experimental binding energies of the PR inhibitors were compared to the ONIOM calculated results. The theoretical binding free energies (ΔG_{bind}) for subtype B follow a similar trend to the experimental results, with one exemption. The computational model was less suitable for C-SA PR. Analysis of the results provided valuable information about the shortcomings of this approach. Future studies will focus on the improvement of the computational model by considering explicit water molecules in the active pocket. We believe that this approach has the potential to provide much improved binding energies for complex enzyme drug interactions.

1. Introduction

Acquired immune deficiency syndrome (AIDs) caused by the Human immune virus (HIV) remains a major disease worldwide, mostly in Africa. The illness was first discovered in the 80′s by Luc Montagnier [1,2] and further categorized by Gallo et al [3]. The size of infected population and the number of HIV patients increase yearly and this has become a major health concern [4]. The human immune virus is classified into two main types (HIV-type 1 and HIV-type 2); type 1 is further categorize into ten subtypes [5–7], of which subtype C-SA is prevalent in South Africa (95%) [5,8–10]. The active form of the HIV-1 protease consists of C2-symmentric, identical 99-amino acids homodimer, bonded by hydrophobic and electrostatic forces as well as hydrogen bonds [11,12].

The HIV-1 aspartic protease active site is composed of Asp25-Thr26-Gly27 catalytic triads enclosed by an extended two glycine rich β-sheets hairpins known as flaps [7,13]. The triads are located at the edge of substrate binding site, and support the catalysis cleavage (especially the ASP) of the scissile substrate peptide [10,14,15].

Antiviral inhibitors were developed against HIV-1 protease as it was considered to be the most eminent target [16,17]. A number of HIV-1 protease antiretroviral drugs approved by the FDA, were developed for subtype B, which is the more common strain found in Australia, Western Europe and North America. These drugs exhibit weaker activities against subtype C and A found in sub-Sahara Africa and India [6–8].

The single crystal X-ray structure of the South African HIV-1 protease subtype C (C-SA HIV-1 PR) [18] was resolved and a successful modelling of this enzyme based on the peptide sequence has also been reported by our group [19–21]. Experimental binding free energies for C-SA HIV PR have previously only been determined for four of the FDA approved protease inhibitors [8,22]. Recently, our laboratory determined the binding free energies for all nine approved HIV PR drugs against C-SA HIV PR [23].

* Corresponding authors at: Catalysis and Peptide Research Unit, School of Health Sciences, University of KwaZulu-Natal, Durban 4041, South Africa.
E-mail addresses: kruger@ukzn.ac.za (H.G. Kruger), Honarparvar@ukzn.ac.za (B. Honarparvar).

http://dx.doi.org/10.1016/j.jmgm.2017.06.026
1093-3263/

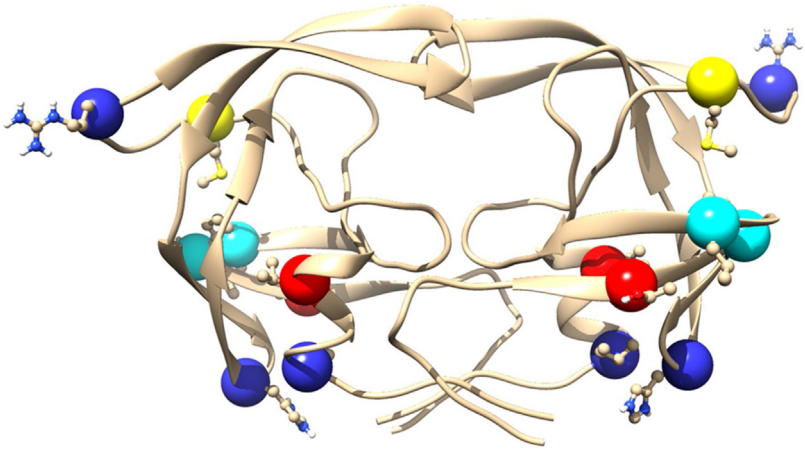

Fig. 1. Homo dimeric X-ray structure of subtype C-SA protease (PDB code:3U71) [18] adopted in this study, showing the positions occupied by the eight amino acids polymorphism R41K, L19I, T12S, H69K, I93L, I15V, L89M and M36I [8] located outside the active site. This structure was created using chimera [58].

It was demonstrated before [24] that experimental binding free energies (ΔG_{bind}) represent the most suitable comparative index for calculated binding free energies [5,25–27].

The inhibitory activities of a selected number of commercial inhibitors against subtype B/mutants and subtype A, C, and F HIV-1 PRs were investigated using molecular dynamics simulations [7,28]. It was suggested that the HIV-1 PR mutations can alter the energetic and dynamic complexation of the enzyme and this can affect the binding properties of the inhibitors [7] leading to drug resistance. The effect of mutations ultimately leads to drug resistance in the HIV-1 PR causing differences in the binding affinities of the protease inhibitors [28]. Our group also reported the theoretical binding free energies of the FDA approved protease inhibitors against both subtype B and C-SA HIV PRs using molecular dynamics (MM-GBSA) [5,10]. The observed results show that the absolute experimental values versus theoretical values differ due to the available parameterization implemented in the theoretical models which is an approximate of experimental data [29], but still largely follow a similar trend with the experiment particularly for subtype B [5,10].

Our Own N-layered Integrated molecular Orbital and molecular Mechanics (ONIOM) method was developed by Morokuma [30–32]. In this multi-layered approach, the active site is treated with a high level of theory (Density Functional Theory or Ab Initio) while the rest of the system/enzyme is treated at a lower level (AMBER). This hybrid approach allows for treatment of large molecular systems in different research areas [33–36]. Several studies have utilized the ONIOM model for calculating interaction energies of wild-type HIV PR-1 with selected commercial inhibitors [37–39]. In all cases, the catalytic aspartate residue was treated at high level of theory, B3LYP/6-31G(d,p) and the rest of the system was modeled at MM level of theory. The binding free energies derived from the ONIOM model were compared with other binding energies derived by different computational approaches. It was concluded from the results obtained that the choice of the protonation state of the Asp dyad has an effect on the dynamic behavior of the enzyme [37–39]. The choice of protonation state for the catalytic HIV PR aspartates (Asp 25/25′) for ONIOM calculations has been studied extensively in literature [20,21,40–42]. It can be concluded that the p*K*a of one of the catalytic aspartate increases to 5.2 [15] when bound to the inhibitor; the corresponding value is p*K*a 4.5 [43] when unbound [44]. This implies that one of the two catalytic Asp groups should be protonated for binding studies, while the other Asp is unprotonated [24].

In other enzymatic studies, the ONIOM approach was extensively used to calculate the binding free energies of ligand—protein interactions at the B3LYP/6-31G(d):MM level of theory [34,45,46]. Comparison of the computed ONIOM results of the high and low potent inhibitors (−111.7 and −112.3 kcal/mol) with the reported K_d experimental dissociation constants (1.1–29 nM) indicated that the two-layer ONIOM binding energies are not always supported by experimental findings [35]. The inconsistency in the calculated ONIOM energies and experimental dissociation constants was attributed to the selected layer for the QM region in the two-layer ONIOM calculations [35].

In this study, a QM:MM two-layer ONIOM hybrid method was adopted to investigate the binding affinity of the FDA approved protease drugs against subtype B and C-SA HIV-1 protease. For further analysis of the obtained ONIOM binding free energies, we investigated the thermodynamic parameters, electrostatic and hydrogen bonding interactions for these inhibitor—enzyme complexes.

2. Materials and methods

The X-ray crystal structures for the nine commercial protease drugs complexed with subtype B HIV PR have been reported: 4YOA (DRV) [47], 4L1A (LPV) [48], 4EYR (RTV) [49], 3WSJ (IDV) [50], 3S56 (SQV) [51], 3S45 (APV) [51], 2PYM (NFV) [52], 4NJU (TPV) [53], 3EM4 (ATV) [54] (Fig. 2). C-SA HIV PR (PDB code: 3U71) [18] is different at eight point amino acids residue mutations with respect to subtype B (PDB code:1HXW) [55]: R41K, L19I, T12S, H69K, I93L, I15V, L89M and M36I [8] (Fig. 1). Structural preparation of subtype C-SA HIV PR complexed with the nine drugs were performed as reported before [5,10], since the X-ray structures for C-SA PR complexed with the FDA approved drugs have not yet been recorded in the Protein Data Bank (PDB). Further structural analysis were performed on these complexes to evaluate the mode of interactions between the ligands and the corresponding subtype B and C-SA HIV PRs using Ligplot [56] and Accelrys (Discovery) Visualizer [57] software.

Based on the reported protonation state [20,21,40–42] of the HIV PR, a mono-protonated Asp 25/25′ state was induced in the binding site at physiological pH 7. The protonation state of both HIV enzymes adopted in this study were assigned using PROPKA [59,60] based on standard p*K*a values at pH 7. It is notable that all the Asp, Glu, Lys, Arg amino acids with the C and N-terminal groups were also charged, whereas His was kept in its neutral form [39].

To ensure that the selected inhibitors maintains the same pose inside the binding site of the subtype C-SA as the subtype B protease, the C-SA PR were superimposed with the subtype B HIV PR—inhibitor crystal complexes using PyMOL [61]. The PyMOL measures the root mean square (RMS) of the superimposed struc-

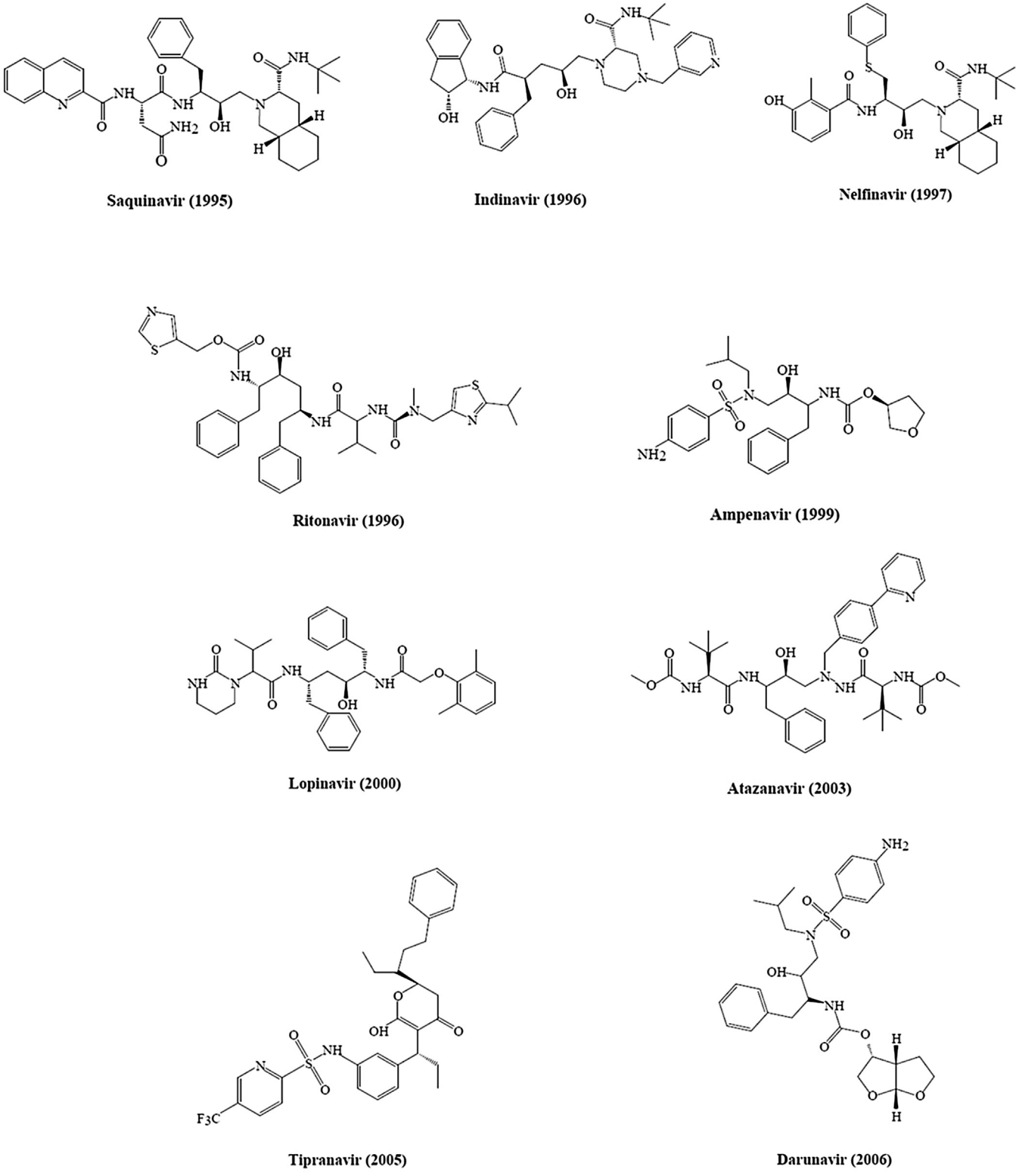

Fig. 2. The structures of HIV-1 FDA approved protease inhibitors [5,10,74,75].

tures, which indicates how well the inhibitor—enzyme complexes were superimposed. An optimal superimposition is recognized if the RMS is less than 2 Å [62–64].

The structures of all inhibitor—enzyme complexes were refined afterwards by removing the ions and crystallographic water, that are present from the protein manually from the PDB file using a text editor. Thereafter, protons were added to the required catalytic aspartate using GaussView [65]. The active Asp25/25′ residues and the inhibitors were considered at a high level (QM/DFT [66,67] – B3LYP [68,69]/6-31G(d) [70,71]) and the remaining part of the system at low layer (MM – AMBER [72]) for subsequent ONIOM [32,73] calculations.

Superimposed structures of all the subtype C-SA HIV PR—inhibitor complexes are provided with the Supplementary

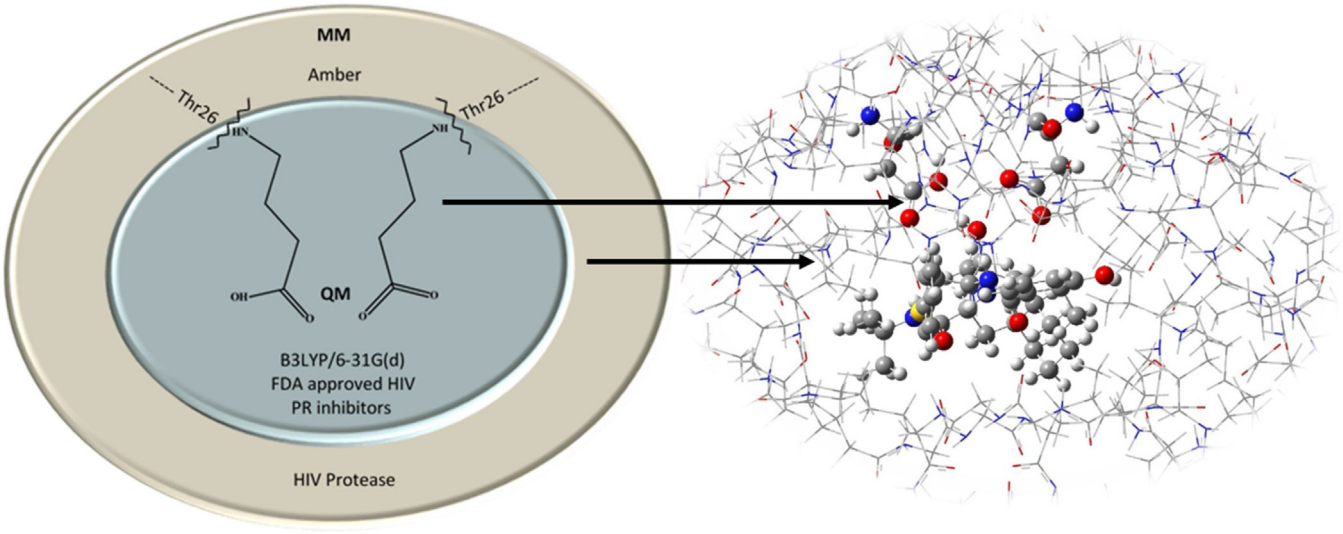

Fig. 3. Schematic diagram of the two-layered ONIOM model (B3LYP/6-31G(d):AMBER) of subtype C-SA—NFV HIV PR complex.

material Fig. S1. The ONIOM input files as well as the optimized output files of all inhibitor—enzyme complexes are also provided in PDB format with the Supplementary materials.

2.1. ONIOM binding free energies

A two-layer ONIOM [31,76,77] approach was applied to calculate the binding free energies of the different PR drugs with the subtype B and C-SA HIV PR. Preceding studies showed that the Becke3LYP method gives better relative energies and are in agreement with high level ab-initio methods [45,78,79]. Hence, full optimization calculations were carried out on both the ligands and inhibitor—enzyme complexes with Gaussian09 package [80], using ONIOM (B3LYP/6-31G(d):AMBER) for the QM:MM level of theory. A schematic illustration of the ONIOM2 model is depicted in Fig. 3.

The total interaction energy attained from the ONIOM2 calculations [81,82] is defined as:

$$\Delta E_{ONIOM} = \Delta E_{model,high} + \Delta E_{real,low} - \Delta E_{model,low} \quad (1)$$

Where, ΔE_{model} is the energies of the model system calculated at the high and low level respectively and ΔE_{real} presents the energy of the entire (real) system.

The relative standard Gibbs free energies (ΔG) of all reactions, were derived from the frequency calculations at ONIOM (B3LYP/6-31G(d):AMBER) QM:MM level of theory. Thus, the corresponding binding free ONIOM energies of the complex systems are calculated from:

$$\Delta G_{ONIOM} \approx \Delta G_{bind} = G_{complex} - G_{protein} - G_{ligand} \quad (2)$$

The thermodynamics quantities (enthalpy and entropy) changes were also obtained from the ONIOM calculation within the enzyme system for C-SA HIV PR. The entropy (ΔS) of all the reactions is estimated by a thermodynamic equation [83].

$$\Delta S_{total} = \Delta S_{surroundings} + \Delta S_{system} \quad (3)$$

$$\Delta S_{total} = \Delta S_{translational} + \Delta S_{vibrational} + \Delta S_{rotational} \quad (4)$$

3. Results and discussion

The RMS values of the superimposed inhibitor—enzyme complexes observed were in the range of 0.5–0.8 Å for all the 18 systems set up for this study (Fig. 4), which shows a reasonably good superimposed prediction [62–64]. Visual inspection was also performed to compare the initial inhibitor—enzyme complex conformation before and after optimization. In each optimization process, it was observed that the selected inhibitors remained inside the active pocket of the individual subtype B and C-SA HIV PRs as the starting X-ray structures.

The ONIOM binding free energies for subtype B and C-SA HIV PRs with the various FDA approved drugs are reported in Table 1. The experimental Gibbs energies for the aforementioned complexes [22,25–27] were used to evaluate the accuracy of our theoretical model. It was stated above, that the parameterization available in theoretical models which is an approximate of experimental data creates a considerable difference between the experimental values and theoretical values [29]. This fact was also observed in earlier studies where the binding free energies derived by MD/MM-GBSA method was compared with the experimental data [5,9,10]. Likewise, the same difference with respect to the experimental data was also observed in our calculated results using the two-layer ONIOM model, however, the observed trend in the theoretical and experimental data are similar and informative.

It is evident from the compiled experimental data that the second generation protease inhibitors (DRV, TPV, ATV, and LPV) show better binding affinities compared to the first generation (APV, SQV, RTV, NFV, IDV) against subtype B protease. However, for subtype C-SA PR the only second generation inhibitor that demonstrates an improved binding free energy is ATV.

Likewise, our calculated ONIOM (B3LYP/6-31G(d):AMBER) binding free energies for subtype B reveal better binding affinities for the second generation inhibitors. The calculated energy for ATV is considerably more negative (−85.3 kcal/mol) than other inhibitors complexed to the enzyme and the reasons are discussed afterwards. The rest of the theoretical binding free energies for subtype B follow the same trend as the experimental energies (Table 1).

For C-SA HIV PR there are two exemptions (outliers): TPV (−78.9 kcal/mol) and NFV (−38.6 kcal/mol), unlike for subtype B, there appears to be no clear correlation between the trend of the calculated binding free energies and the reported experimental energies [23]. In the previous report for a two-layer ONIOM model, it was realized that the general trend for theoretical binding energies does not always correlate with experimental data [35]. Despite the uncertain correlation, the following more general observation was made for both experimental and computed binding energies for C-SA PR. ATV, APV, IDV, RTV, and DRV exhibit comparable better

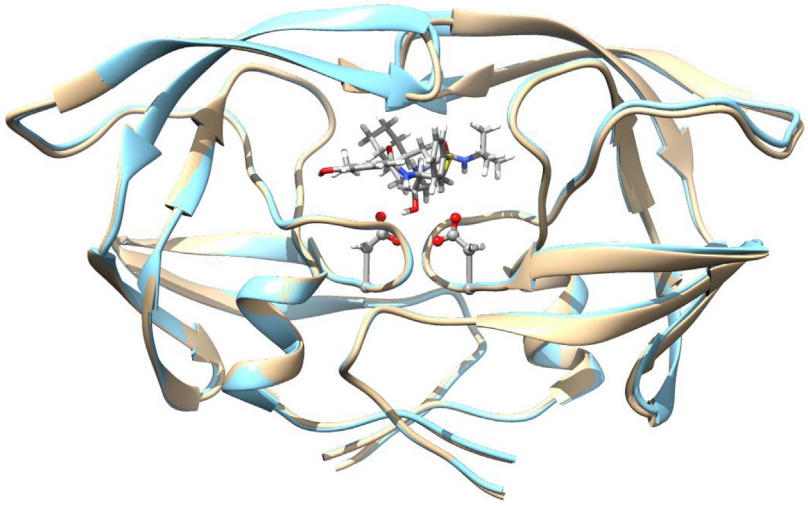

Fig. 4. Super-imposed inhibitor—enzyme complex of subtype B—NFV (blue) with C-SA PR (brown). This structure was created using PyMOL [61]. (For interpretation of the references to colour in this figure legend, the reader is referred to the web version of this article.)

Table 1
The binding free energies (kcal mol^{-1}) for HIV PIs against Subtype B and C-SA obtained by ONIOM (B3LYP/6-31G(d):AMBER).

Inhibitors	ΔG_{bind} values for Subtype B kcal/mol		ΔG_{bind} values for Subtype C-SA kcal/mol	
First generation PIs				
	Exp[a]	Theory[b]	Exp[c]	Theory[b]
RTV	−13.7	−62.8	−13.9	−62.9
APV	−13.2	−56.4	−13.9	−69.0
SQV	−13.0	−54.0	−13.4	−57.1
NFV	−12.8	−46.2	−13.5	−38.6
IDV	−12.4	−45.8	−14.0	−64.0
Second generation PIs				
DRV	−15.2	−65.9	−13.8	−62.8
LPV	−15.1	−65.7	−13.2	−56.5
TPV	−14.6	−63.1	−13.2	−78.9
ATV	−14.3	−85.3	−14.4	−66.9

Note: HIV protease inhibitors are ranked in terms of their binding free energies. The ONIOM (Gaussian) input files as well as the optimized output files of all inhibitor—enzyme complexes are also provided in PDB format with the Supplementary material.

[a] Experimental binding Gibbs free energies taken from literature against subtype B PR [5,22,25–27].

[b] Calculated binding free energies using ONIOM for subtype B and C-SA PR respectively.

[c] Experimental binding Gibbs free energies taken from literature against subtype C-SA PR [23].

binding affinities, while SQV, LPV and NFV revealed weaker binding affinities.

Several factors can potentially contribute to the different results for the two enzymes adopted in this study. First, there are eight point mutations in C-SA compared with subtype B HIV PR [8]. The experimental study for subtype B and the first resolved crystal structure for subtype C-SA protease divulge that polymorphisms at residue 36 of the C-SA HIV PR have a significant influence on the stability of the enzyme hinge region. Also, the lack of the E35-R57 salt bridge results in reduced stability of the hinge region; the latter contributes to increased flaps flexibility [18] and the flap movement plays a major role in the complexation event and thus the binding free energies[84–86].

Subsequently, an attempt was made to achieve further insight into the detailed hydrogen bond interactions of the inhibitor—enzyme complexes. The hydrogen bond distances were measured between both catalytic aspartates in the active pocket and hydroxyl group of the selected FDA approved inhibitors. All the inhibitor—enzyme interactions were plotted using Accelrys (Discovery) Visualizer [57] before and after optimization.

Comparison of the average hydrogen bond (HB) distances between active residues of subtype B and C-SA PR with the selected ligands, shows that in all cases, the hydroxyl group of the inhibitors form hydrogen bonding with Asp25/25′ of HIV proteases (Fig. 5).

The change in hydrogen bond distances between the inhibitor —OH group and Asp 25/25′ were calculated (Fig. S3, Supplementary material) for all the inhibitor—enzyme complex structures before and after optimization. For subtype B, the first generation inhibitors (with weaker binding energies) experience a slight reduction in the average hydrogen bond distance of 0.1 Å. While, the second generation inhibitors (with better binding energies) revealed a larger reduction with an average hydrogen bond distance of 0.5 Å upon optimization of the inhibitor—enzyme complex. When the optimized inhibitor —OH and Asp25/25′ hydrogen bond distances for subtype B/TPV (3.3 Å; −63.1 kcal/mol) are compared to that of the outlier subtype B/ATV complex (1.7 Å; −85.3 kcal/mol). It is clear that ATV experiences a much stronger hydrogen bond interaction, most likely leading to the increased theoretical binding free energy.

In the case of the subtype C-SA PR outliers: For TPV, comparison of the hydrogen bond distances with ATV reveal that TPV (3.1 Å; −78.9 kcal/mol) has a stronger hydrogen bond interaction than ATV (4.4 Å; −66.9 kcal/mol). This also explains the difference in calculated binding free energies of these two complexes. For the other C-SA outlier: NFV, a comparison with SQV that has a similar experimental binding free energy, the corresponding hydrogen bond distance for NFV (4.4 Å; −38.6 kcal/mol) is longer than that of SQV (4.1 Å; −57.1 kcal/mol). This greater distance for NFV corresponds to a weaker theoretical binding free energy.

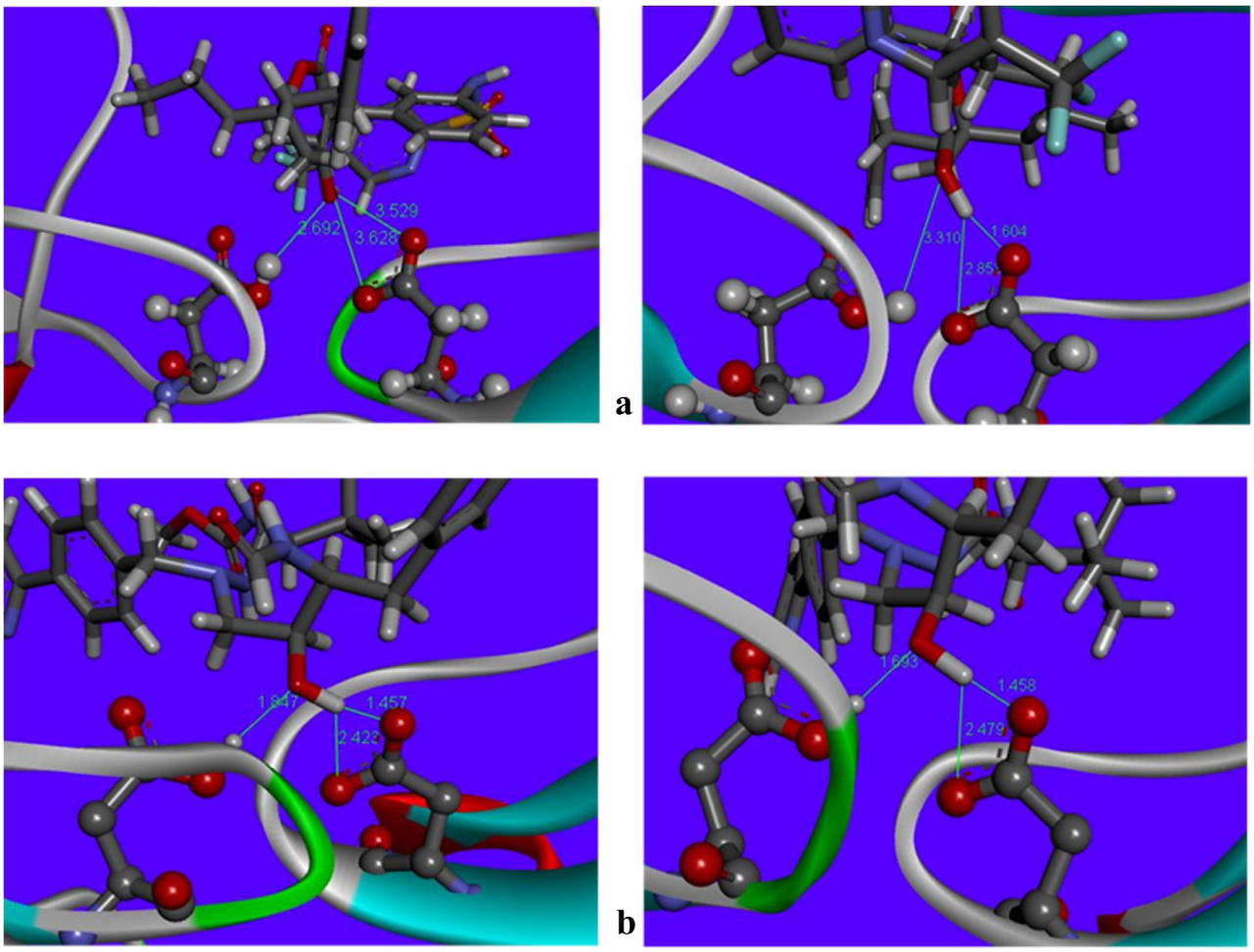

Fig. 5. Hydrogen bond distances between the hydroxyl groups of the TPV and ATV drugs with the catalytic ASP25 and ASP25' residues of a: subtype B—TPV PR, b: subtype B—ATV PR before and after optimization using Accelrys (Discovery) visualizer. Detailed comparative plots for all inhibitor—enzyme complexes are provided with the Supplementary material Fig. S3. (The ONIOM (Gaussian) input files as well as the optimized output files of all inhibitor—enzyme complexes are also provided in PDB format with the Supplementary material.).

To further probe the nature of these differences in calculated binding free energies, the electrostatic and hydrogen bond interactions for both subtype B and C-SA HIV-1 PRs complexed with the various FDA approved inhibitors were plotted using Ligplot [56] and depicted in Fig. 6 (for subtype B—ATV) and in the Supplementary material (Fig. S2). The plots show hydrogen bonding and electrostatic interactions occurring between the inhibitors, catalytic aspartate and other residues in both proteases. However, the mode of interaction differs from subtype B and C-SA PR, this may be due to the polymorphism occurring in C-SA HIV PR which causes the enzyme to be more flexible [18].

The calculated thermochemical properties [binding free interaction energy (ΔG), enthalpy (ΔH) and entropy (ΔS) contributions] of the various drugs complexes with subtype B (Table 2) and C-SA HIV PR are provided in Supplementary material (Table S1).

The calculated binding free energies (ΔG) for the various FDA approved inhibitors complexes with subtype B follow the same trend as the experimental data (Table 1), except for ATV, while the C-SA HIV PR has two outliers (TPV and NFV) as discussed earlier. The thermochemical properties can be used to explain these outliers since ΔG is a function of both enthalpy (ΔH) and entropy (ΔS).

For the subtype B outlier, ATV: the ΔH value (−104.2 kcal/mol) (Table 2) suggests a better binder than the rest of the drugs complexed to the enzyme. As demonstrated before, this may arise from stronger hydrogen bond interactions between the ATV hydroxyl group and the catalytic aspartate residue, which translates into a larger binding free energy ΔG (−85.3 kcal/mol).

For the two C-SA, outliers TPV and NFV (Table S1, Supplementary material), it is noticeable that the ΔH (−129.3 kcal/mol) for TPV also suggests better binding energy than the rest of the drugs in complex with the enzyme. While ΔH (−59.3 kcal/mol) for NFV indicates a weaker contact. These enthalpy values are attributed to the nature of the hydrogen bond interaction between the inhibitor —OH group and the catalytic aspartate (Fig. 5 and subsequent discussion). Thus, it reflects a stronger binding free energy ΔG (−78.9 kcal/mol) for TPV and a weaker binding free energy ΔG (−38.6 kcal/mol) for NFV.

For the various FDA approved drugs, it should be noted that more negative entropies (higher entropy penalty) is indicative of greater restrictions of movement for the ligand in the active site, due to stronger non-covalent inhibitor—enzyme interactions for certain parts of the inhibitor [87]. The translational and rotational entropy contributions are in close range for both subtype B and C-SA HIV PRs (Table S1), it can be seen that the major entropy contribution is from the vibrational energy component. LPV demonstrates a larger entropy penalty ΔS_{total} (−113.2 cal/mol K) for the subtype B than any of the other inhibitors. An entropy penalty is normally paid upon restriction of the inhibitor [87] and in this case most possibly due to stabilization of the ligand side chains. Hydrogen bond interactions occur for two side chain residues of LPV with amino acids

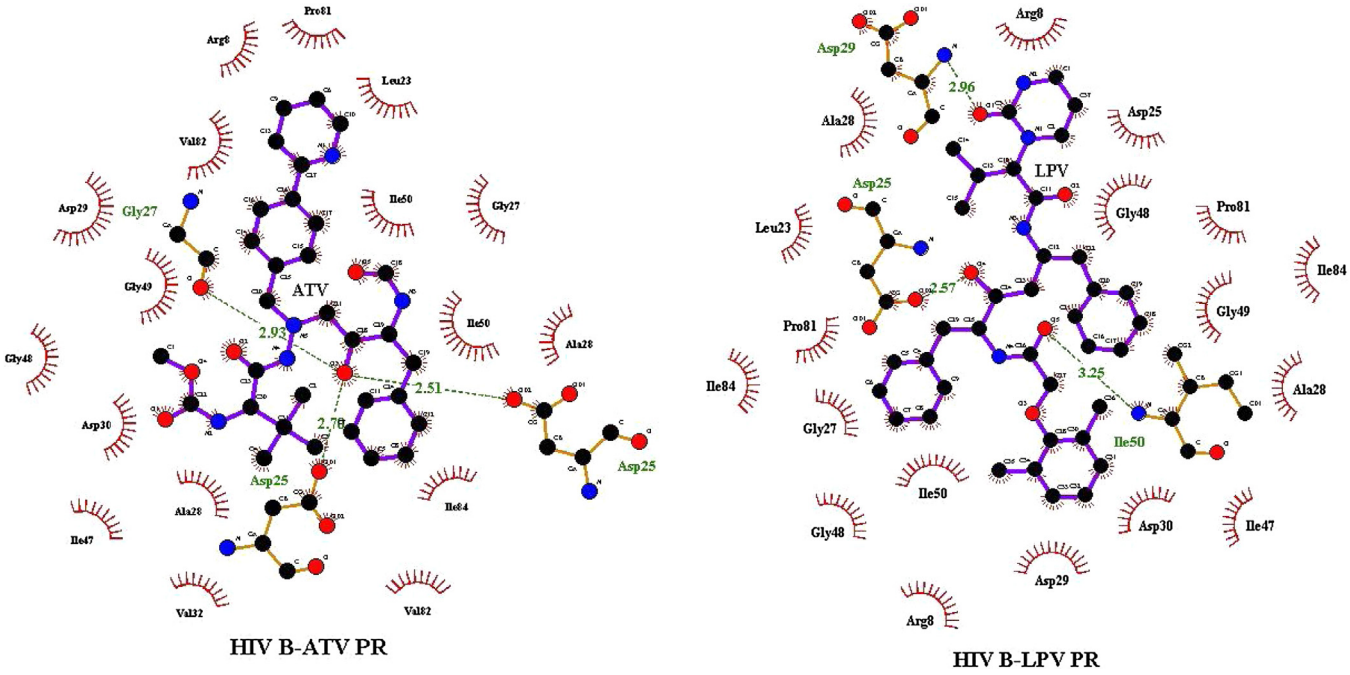

Fig. 6. Electrostatic and hydrogen bond interactions plot of HIV subtype B PR complexed with ATV and LPV. These plots were created after ONIOM optimization of each complex system using Ligplot [56]. Detailed plots showing the electrostatic and hydrogen bond interactions for the remaining complexes are provided with the Supplementary material Fig. S2. (The ONIOM (Gaussian) input files as well as the optimized output files of all inhibitor—enzyme complexes are also provided in PDB format with the Supplementary material.

Table 2
The binding free energies, enthalpies and entropy of the various FDA approved HIV PIs against subtype B PR.

Inhibitors	ΔG^a kcal mol^{-1}	ΔH kcal mol^{-1}	ΔS_{total} cal mol^{-1} K^{-1}	ΔS_{trans} cal mol^{-1} K^{-1}	ΔS_{vib} cal mol^{-1} K^{-1}	ΔS_{rot} cal mol^{-1} K^{-1}
		First generation PIs				
RTV	−62.8	−70.5	−25.1	−43.9	56.8	−38.1
APV	−56.4	−81.8	−85.4	−44.5	−3.3	−37.6
SQV	−54.0	−70.1	−53.3	−45.3	31.3	−39.3
NFV	−46.2	−58.5	−41.4	−44.8	41.6	−38.2
IDV	−45.8	−67.8	−71.4	−45.0	12.9	−39.3
		Second generation PIs				
DRV	−65.9	−76.8	−37.2	−43.1	42.1	−36.3
LPV	−65.7	−99.7	−113.2	−43.5	−32.5	−37.2
TPV	−63.1	−75.1	−39.9	−43.4	41.2	−37.6
ATV	−85.3	−104.2	−63.3	−43.2	16.3	−36.5

HIV protease inhibitors (HIV PIs) are ranked in terms of their binding free energies (ΔG), the thermodynamics values for subtype C-SA are provided with Supplementary material (Table S1). The ONIOM (Gaussian) input files as well as the optimized output files of all inhibitor—enzyme complexes are also provided in PDB format with the Supplementary material.

[a] Calculated binding free energies using ONIOM for subtype B PR (taken from Table 1).

in the active site of the enzyme (Fig. 5), which explain the observed increase in entropy value for LPV (Table 2). These restrictions were not observed to the same extend for the other inhibitors.

The calculated binding free energies of the FDA approved drugs against subtype B in comparison to C-SA HIV PR, reveals that the model works better for subtype B. The outlier results for subtype B and C-SA PR appears to be due to the approximations applied in our ONIOM model. Movement of the inhibitors closer to the Asp25/25′ residues during optimization, suggest that omission of water molecules in the model is an over-simplification and should be addressed in future studies.

4. Conclusion

In this study, the binding free energies of the nine selected HIV-1 PR inhibitors were investigated using a two-layered ONIOM (B3LYP/6-31G(d):AMBER) model. The difference in binding affinities of the PIs with the two proteases seems to relate to the insertion and mutants experienced by the mutant and the extent of binding interactions between the catalytic aspartates, Asp25/25′, and the inhibitors.

The calculated binding free energies for subtype B HIV PR show a satisfactory trend with the experimental data with one exception. For subtype C-SA HIV PR, some discrepancies occur in terms of the trend with the experimental data, which means that the existing model requires further optimization before it can be used for C-SA PR.

It is known that water molecules facilitate the catalytic interactions of the substrate with the Asp 25/25′ residues, therefore the level of accuracy of the two layer ONIOM model can be improved by adding explicit water molecules to the active site of the HIV PR and in the least treated at a semi-empirical level (PM6). The information obtained from this research is helpful to improve the computational model for the potential design of more potent C-SA HIV PR inhibitors.

Competing interests

The authors declare that they have no competing interests.

Author contributions

Z.K. Sanusi (masters student, computational work), T. Govender (supervisor biochemistry work), G.E.M. Maguire (supervisor computational chemistry), S. B. Maseko (PhD biochemistry work), J. Lin (supervisor biochemistry work), H. G. Kruger* (supervisor computational chemistry) and B. Honarparvar* (supervisor computational chemistry).

Acknowledgments

We thank the College of Health Sciences (CHS), Aspen Pharmacare, MRC and the NRF for financial support. We are also grateful to the CHPC (www.chpc.ac.za) and UKZN HPC cluster as our computational resources.

Appendix A. Supplementary data

Supplementary data associated with this article can be found, in the online version, at http://dx.doi.org/10.1016/j.jmgm.2017.06.026.

References

[1] M. Shehu-Xhilaga, R. Oelrichs, Basic HIV Virology, HIV Management in Australasia, 2009, pp. 9–18.
[2] D. Klatzmann, E. Champagne, S. Chamaret, J. Gruest, D. Guetard, T. Hercend, J.-C. Gluckman, L. Montagnier, T-lymphocyte T4 molecule behaves as the receptor for human retrovirus LAV, Nature 312 (1983) 767–768.
[3] R.C. Gallo, P.S. Sarin, E. Gelmann, M. Robert-Guroff, E. Richardson, V. Kalyanaraman, D. Mann, G.D. Sidhu, R.E. Stahl, S. Zolla-Pazner, Isolation of human T-cell leukemia virus in acquired immune deficiency syndrome (AIDS), Science 220 (1983) 865–867.
[4] HIV/AIDS, J.U.N.P.o., and HIV/AIDS, J.U.N.P.o. (2016) Global AIDS update 2016, Geneva, Switzerland.
[5] S.M. Ahmed, H.G. Kruger, T. Govender, G.E. Maguire, Y. Sayed, M.A. Ibrahim, P. Naicker, M.E. Soliman, Comparison of the molecular dynamics and calculated binding free energies for nine FDA-approved HIV-1 PR drugs against subtype B and C-SA HIV PR, Chem. Biol. Drug Des. 81 (2013) 208–218.
[6] A.H. Robbins, R.M. Coman, E. Bracho-Sanchez, M.A. Fernandez, C.T. Gilliland, M. Li, M. Agbandje-McKenna, A. Wlodawer, B.M. Dunn, R. McKenna, Structure of the unbound form of HIV-1 subtype A protease: comparison with unbound forms of proteases from other HIV subtypes, Acta Crystallogr. Sect. D: Biol. Crystallogr. 66 (2010) 233–242.
[7] A. Genoni, G. Morra, K.M. Merz Jr., G. Colombo, Computational study of the resistance shown by the subtype B/HIV-1 protease to currently known inhibitors, Biochemistry 49 (2010) 4283–4295.
[8] S. Mosebi, L. Morris, H.W. Dirr, Y. Sayed, Active-site mutations in the South African human immunodeficiency virus type 1 subtype C protease have a significant impact on clinical inhibitor binding: kinetic and thermodynamic study, J. Virol. 82 (2008) 11476–11479.
[9] S.M. Ahmed, G.E. Maguire, H.G. Kruger, T. Govender, The impact of active site mutations of South African HIV PR on drug resistance: insight from molecular dynamics simulations, binding free energy and per-residue footprints, Chem. Biol. Drug Des. 83 (2014) 472–481.
[10] H.A. Lockhat, J.R. Silva, C.N. Alves, T. Govender, J. Lameira, G.E. Maguire, Y. Sayed, H.G. Kruger, Binding free energy calculations of nine FDA-approved protease inhibitors against HIV-1 subtype C I36T↑ T containing 100 amino acids per monomer, Chem. Biol. Drug Des. 87 (2015) 487–498.
[11] A.S. Braz, P. Tufanetto, D. Perahia, L.P. Scott, Relation between flexibility and positively selected HIV-1 protease mutants against inhibitors, Proteins: Struct. Funct. Bioinform. 80 (2012) 2680–2691.
[12] C. Bonini, L. Chiummiento, M. De Bonis, N. Di Blasio, M. Funicello, P. Lupattelli, R. Pandolfo, F. Tramutola, F. Berti, Synthesis of new thienyl ring containing HIV-1 protease inhibitors: promising preliminary pharmacological evaluation against recombinant HIV-1 proteases, J. Med. Chem. 53 (2010) 1451–1457.
[13] L. Vangelista, M. Secchi, P. Lusso, Rational design of novel HIV-1 entry inhibitors by RANTES engineering, Vaccine 26 (2008) 3008–3015.
[14] R. Kurth, N. Bannert, Retroviruses: Molecular Biology, Genomics and Pathogenesis, Horizon Scientific Press, 2010.
[15] A. Brik, C.-H. Wong, HIV-1 protease: mechanism and drug discovery, Org. Biomol. Chem. 1 (2003) 5–14.
[16] H.M. Abdel-Rahman, G.S. Al-karamany, N.A. El-Koussi, A.F. Youssef, Y. Kiso, HIV protease inhibitors: peptidomimetic drugs and future perspectives, Curr. Med. Chem. 9 (2002) 1905–1922.
[17] A. Wlodawer, Rational approach to AIDS drug design through structural biology, Annu. Rev. Med. 53 (2002) 595–614.
[18] P. Naicker, I. Achilonu, S. Fanucchi, M. Fernandes, M.A. Ibrahim, H.W. Dirr, M.E. Soliman, Y. Sayed, Structural insights into the South African HIV-1 subtype C protease: impact of hinge region dynamics and flap flexibility in drug resistance, J. Biomol. Struct. Dyn. 31 (2013) 1370–1380.
[19] M.M. Makatini, K. Petzold, C.N. Alves, P.I. Arvidsson, B. Honarparvar, P. Govender, T. Govender, H.G. Kruger, Y. Sayed, Jerônimo Lameira, Synthesis, 2D-NMR and molecular modelling studies of pentacycloundecane lactam-peptides and peptoids as potential HIV-1 wild type C-SA protease inhibitors, J. Enzyme Inhib. Med. Chem. 28 (2013) 78–88.
[20] R. Karpoormath, Y. Sayed, P. Govender, T. Govender, H.G. Kruger, M.E. Soliman, G.E. Maguire, Pentacycloundecane derived hydroxy acid peptides: a new class of irreversible non-scissile ether bridged type isoster as potential HIV-1 wild type C-SA protease inhibitors, Bioorg. Chem. 40 (2012) 19–29.
[21] B. Honarparvar, M.M. Makatini, S.A. Pawar, K. Petzold, M.E. Soliman, P.I. Arvidsson, Y. Sayed, T. Govender, G.E. Maguire, H.G. Kruger, Pentacycloundecane-diol-based HIV-1 protease inhibitors: biological screening, 2D NMR, and molecular simulation studies, ChemMedChem 7 (2012) 1009–1019.
[22] A. Velazquez-Campoy, S. Vega, E. Freire, Amplification of the effects of drug resistance mutations by background polymorphisms in HIV-1 protease from African subtypes, Biochemistry 41 (2002) 8613–8619.
[23] S.B. Maseko, E. Padayachee, T. Govender, Y. Sayed, G. Kruger, G.E. Maguire, J. Lin, I36T↑ T mutation in South African subtype C (C-SA) HIV -1 protease significantly alters protease-drug interactions, Biol Chem (2017), http://dx.doi.org/10.1515/hsz-2017-0107.
[24] B. Honarparvar, T. Govender, G.E. Maguire, M.E. Soliman, H.G. Kruger, Integrated approach to structure-based enzymatic drug design: molecular modeling, spectroscopy, and experimental bioactivity, Chem. Rev. 114 (2013) 493–537.
[25] H. Ohtaka, A. Velázquez-Campoy, D. Xie, E. Freire, Overcoming drug resistance in HIV-1 chemotherapy: the binding thermodynamics of amprenavir and TMC-126 to wild-type and drug-resistant mutants of the HIV-1 protease, Protein Sci. 11 (2002) 1908–1916.
[26] N.M. King, M. Prabu-Jeyabalan, E.A. Nalivaika, P. Wigerinck, M.-P. de Béthune, C.A. Schiffer, Structural and thermodynamic basis for the binding of TMC114, a next-generation human immunodeficiency virus type 1 protease inhibitor, J. Virol. 78 (2004) 12012–12021.
[27] S. Muzammil, A. Armstrong, L. Kang, A. Jakalian, P. Bonneau, V. Schmelmer, L. Amzel, E. Freire, Unique thermodynamic response of tipranavir to human immunodeficiency virus type 1 protease drug resistance mutations, J. Virol. 81 (2007) 5144–5154.
[28] P.R. Batista, A. Wilter, E.H. Durham, P.G. Pascutti, Molecular dynamics simulations applied to the study of subtypes of HIV-1 protease common to Brazil, Africa, and Asia, Cell Biochem. Biophys. 44 (2006) 395–404.
[29] A. Frisch, J. Foresman, Exploring Chemistry with Electronic Structure Methods, Gaussian Inc., Pittsburgh, PA, 1996, pp. 302.
[30] K. Morokuma, New challenges in quantum chemistry: quests for accurate calculations for large molecular systems, Philos. Trans. R. Soc. Lond. A: Math. Phys. Eng. Sci. 360 (2002) 1149–1164.
[31] S. Dapprich, I. Komáromi, K.S. Byun, K. Morokuma, M.J. Frisch, A new ONIOM implementation in Gaussian98. Part I. The calculation of energies, gradients, vibrational frequencies and electric field derivatives, J. Mol. Struct. THEOCHEM 461 (1999) 1–21.
[32] T. Vreven, K. Morokuma, On the application of the IMOMO (integrated molecular orbital+ molecular orbital) method, J. Comput. Chem. 21 (2000) 1419–1432.
[33] F. Zheng, C.-G. Zhan, Rational design of an enzyme mutant for anti-cocaine therapeutics, J. Comput. Aided Mol. Des. 22 (2008) 661–671.
[34] V. Ruangpornvisuti, Recognition of carboxylate and dicarboxylates by azophenol-thiourea derivatives: a theoretical host-guest investigation, J. Mol. Struct. THEOCHEM 686 (2004) 47–55.
[35] P.N. Samanta, K.K. Das, Prediction of binding modes and affinities of 4-substituted-2,3,5,6-tetrafluorobenzenesulfonamide inhibitors to the carbonic anhydrase receptor by docking and ONIOM calculations, J. Mol. Graph. Modell. 63 (2016) 38–48.
[36] S. Promsri, P. Chuichay, V. Sanghiran, V. Parasuk, S. Hannongbua, Molecular and electronic properties of HIV-1 protease inhibitor C 60 derivatives as studied by the ONIOM method, J. Mol. Struct. THEOCHEM 715 (2005) 47–53.
[37] P. Fong, J.P. McNamara, I.H. Hillier, R.A. Bryce, Assessment of QM/MM scoring functions for molecular docking to HIV-1 protease, J. Chem. Inf. Model. 49 (2009) 913–924.
[38] S. Saen-oon, O. Aruksakunwong, K. Wittayanarakul, P. Sompornpisut, S. Hannongbua, Insight into analysis of interactions of saquinavir with HIV-1 protease in comparison between the wild-type and G48V and G48V/L90M mutants based on QM and QM/MM calculations, J. Mol. Graph. Modell. 26 (2007) 720–727.
[39] K. Wittayanarakul, O. Aruksakunwong, S. Saen-oon, W. Chantratita, V. Parasuk, P. Sompornpisut, S. Hannongbua, Insights into saquinavir resistance in the G48V HIV-1 protease: quantum calculations and molecular dynamic simulations, Biophys. J. 88 (2005) 867–879.

[40] S. Shi, G. Hu, J. Chen, S. Zhang, Q. Zhang, Molecular dynamics simulations on the role of protonation states in HIV-1 protease-indinavir complex, Acta Chim. Sin. 67 (2009) 2791–2797.
[41] Y. Tong, Y. Mei, J.Z. Zhang, L.L. Duan, Q.-G. Zhang, Quantum calculation of protein solvation and protein-ligand binding free energy for hiv-1 protease/water complex, J. Theor. Comput. Chem. 8 (2009) 1265–1279.
[42] M.M. Makatini, Design, Synthesis and Screening of Novel PCU-Peptide/Peptoid Derived HIV Protease Inhibitors, University of KwaZulu-Natal, Westville, 2011.
[43] R. Smith, I.M. Brereton, R.Y. Chai, S.B. Kent, Ionization states of the catalytic residues in HIV-1 protease, Nat. Struct. Mol. Biol. 3 (1996) 946–950.
[44] B. Honarparvar, S.A. Pawar, C.N. Alves, J. Lameira, G.E. Maguire, J.R.A. Silva, T. Govender, H.G. Kruger, Pentacycloundecane lactam vs lactone norstatine type protease HIV inhibitors: binding energy calculations and DFT study, J. Biomed. Sci. 22 (2015) 1–15.
[45] M. Remko, O.A. Walsh, W.G. Richards, Theoretical study of molecular structure, tautomerism, and geometrical isomerism of moxonidine: two-layered ONIOM calculations, J. Phys. Chem. A 105 (2001) 6926–6931.
[46] W. Li, S. Qin, Z. Su, C. Hu, X. Feng, Theoretical study on the mechanism and stereochemistry of salicylaldehyde-Al (III)-catalyzed hydrophosphonylation of benzaldehyde, Comp. Theor. Chem. 989 (2012) 44–50.
[47] B.D. Kuiper, B.J. Keusch, T.G. Dewdney, P. Chordia, K. Ross, J.S. Brunzelle, I.A. Kovari, R. MacArthur, H. Salimnia, L.C. Kovari, The L33F darunavir resistance mutation acts as a molecular anchor reducing the flexibility of the HIV-1 protease 30 s and 80 s loops, Biochem. Biophys. Rep. 2 (2015) 160–165.
[48] Z. Liu, R.S. Yedidi, Y. Wang, T.G. Dewdney, S.J. Reiter, J.S. Brunzelle, I.A. Kovari, L.C. Kovari, Crystallographic study of multi-drug resistant HIV-1 protease lopinavir complex: mechanism of drug recognition and resistance, Biochem. Biophys. Res. Commun. 437 (2013) 199–204.
[49] Z. Liu, R.S. Yedidi, Y. Wang, T.G. Dewdney, S.J. Reiter, J.S. Brunzelle, I.A. Kovari, L.C. Kovari, Insights into the mechanism of drug resistance: X-ray structure analysis of multi-drug resistant HIV-1 protease ritonavir complex, Biochem. Biophys. Res. Commun. 431 (2013) 232–238.
[50] M. Kuhnert, H. Steuber, W.E. Diederich, Structural basis for HTLV-1 protease inhibition by the HIV-1 protease inhibitor indinavir, J. Med. Chem. 57 (2014) 6266–6272.
[51] Y. Tie, Y.F. Wang, P.I. Boross, T.Y. Chiu, A.K. Ghosh, J. Tozser, J.M. Louis, R.W. Harrison, I.T. Weber, Critical differences in HIV-1 and HIV-2 protease specificity for clinical inhibitors, Protein Sci. 21 (2012) 339–350.
[52] M. Kožíšek, J. Bray, P. Řezáčová, K. Šašková, J. Brynda, J. Pokorná, F. Mammano, L. Rulíšek, J. Konvalinka, Molecular analysis of the HIV-1 resistance development: enzymatic activities, crystal structures, and thermodynamics of nelfinavir-resistant HIV protease mutants, J. Mol. Biol. 374 (2007) 1005–1016.
[53] R.S. Yedidi, H. Garimella, M. Aoki, H. Aoki-Ogata, D.V. Desai, S.B. Chang, D.A. Davis, W.S. Fyvie, J.D. Kaufman, D.W. Smith, A conserved hydrogen-bonding network of P2 bis-tetrahydrofuran-containing HIV-1 protease inhibitors (PIs) with a protease active-site amino acid backbone aids in their activity against PI-resistant HIV, Antimicrob. Agents Chemother. 58 (2014) 3679–3688.
[54] N.M. King, M. Prabu-Jeyabalan, R.M. Bandaranayake, M.N. Nalam, E.A. Nalivaika, A.e.l. Özen, T.r. Haliloğlu, N.e.K. Yılmaz, C.A. Schiffer, Extreme entropy-enthalpy compensation in a drug-resistant variant of HIV-1 protease, ACS Chem. Biol. 7 (2012) 1536–1546.
[55] D.J. Kempf, D.W. Norbeck, L. Codacovi, X.C. Wang, W.E. Kohlbrenner, N.E. Wideburg, D.A. Paul, M.F. Knigge, S. Vasavanonda, Structure-based, C2 symmetric inhibitors of HIV protease, J. Med. Chem. 33 (1990) 2687–2689.
[56] R.A. Laskowski, M.B. Swindells, LigPlot+: multiple ligand-protein interaction diagrams for drug discovery, J. Chem. Inf. Model. 51 (2011) 2778–2786.
[57] D. Studio, 4.0 Tutorials, Receptor-Ligand Interaction, Accelrys Inc., San Diego, CA, USA, 2013.
[58] E.F. Pettersen, T.D. Goddard, C.C. Huang, G.S. Couch, D.M. Greenblatt, E.C. Meng, T.E. Ferrin, UCSF chimera—a visualization system for exploratory research and analysis, J. Comput. Chem. 25 (2004) 1605–1612.
[59] H. Li, A.D. Robertson, J.H. Jensen, Very fast empirical prediction and rationalization of protein pKa values, Proteins: Struct. Funct. Bioinform. 61 (2005) 704–721.
[60] http://nbcr-222.ucsd.edu/pdb2pqr_2.0.0/.
[61] W.L. DeLano, The PyMOL Molecular Graphics System, 2002.
[62] J.C. Cole, C.W. Murray, J.W.M. Nissink, R.D. Taylor, R. Taylor, Comparing protein-ligand docking programs is difficult, Proteins: Struct. Funct. Bioinform. 60 (2005) 325–332.
[63] H. Gohlke, M. Hendlich, G. Klebe, Knowledge-based scoring function to predict protein-ligand interactions, J. Mol. Biol. 295 (2000) 337–356.
[64] M. Kontoyianni, L.M. McClellan, G.S. Sokol, Evaluation of docking performance: comparative data on docking algorithms, J. Med. Chem. 47 (2004) 558–565.
[65] R. Dennington, T. Keith, J. Millam, GaussView, Version 5, Semichem Inc., Shawnee, Mission, KS, 2009.
[66] W. Kohn, A.D. Becke, R.G. Parr, Density functional theory of electronic structure, J. Phys. Chem. 100 (1996) 12974–12980.
[67] R. Neumann, R.H. Nobes, N.C. Handy, Exchange functionals and potentials, Mol. Phys. 87 (1996) 1–36.
[68] A.D. Becke, Density-functional thermochemistry. III. The role of exact exchange, J. Chem. Phys. 98 (1993) 5648–5652.
[69] C. Lee, W. Yang, R.G. Parr, Development of the colle-salvetti correlation-energy formula into a functional of the electron density, Phys. Rev. B 37 (1988) 785–789.
[70] P.C. Hariharan, J.A. Pople, The influence of polarization functions on molecular orbital hydrogenation energies, Theor. Chim. Acta 28 (1973) 213–222.
[71] V.A. Rassolov, J.A. Pople, M.A. Ratner, T.L. Windus, 6-31G* basis set for atoms K through Zn, J. Chem. Phys. 109 (1998) 1223–1229.
[72] D.A. Case, T.E. Cheatham, T. Darden, H. Gohlke, R. Luo, K.M. Merz, A. Onufriev, C. Simmerling, B. Wang, R.J. Woods, The Amber biomolecular simulation programs, J. Comput. Chem. 26 (2005) 1668–1688.
[73] T. Vreven, K. Morokuma, Hybrid methods: oniom (QM: MM) and QM/MM, Ann. Rep. Comput. Chem. 2 (2006) 35–51.
[74] J. Vacca, B. Dorsey, W. Schleif, R. Levin, S. McDaniel, P. Darke, J. Zugay, J. Quintero, O. Blahy, E. Roth, L-735,524: an orally bioavailable human immunodeficiency virus type 1 protease inhibitor, Proc. Natl. Acad. Sci. U. S. A. 91 (1994) 4096–4100.
[75] S.W. Kaldor, V.J. Kalish, J.F. Davies, B.V. Shetty, J.E. Fritz, K. Appelt, J.A. Burgess, K.M. Campanale, N.Y. Chirgadze, D.K. Clawson, Viracept (nelfinavir mesylate, AG1343): a potent, orally bioavailable inhibitor of HIV-1 protease, J. Med. Chem. 40 (1997) 3979–3985.
[76] S. Humbel, S. Sieber, K. Morokuma, The IMOMO method: integration of different levels of molecular orbital approximations for geometry optimization of large systems: test for n-butane conformation and SN2 reaction: RCl+ Cl−, J. Chem. Phys. 105 (1996) 1959–1967.
[77] M. Svensson, S. Humbel, R.D. Froese, T. Matsubara, S. Sieber, K. Morokuma, ONIOM: a multilayered integrated MO+ MM method for geometry optimizations and single point energy predictions A test for diels-alder reactions and Pt(P(t-Bu)3)2+ H2 oxidative addition, J. Phys. Chem. 100 (1996) 19357–19363.
[78] J. Kapp, M. Remko, P.v.R. Schleyer, H2XO and (CH3)2XO Compounds (X = C, Si, Ge, Sn, Pb): double bonds vs carbene-like structures can the metal compounds exist at all? J. Am. Chem. Soc. 118 (1996) 5745–5751.
[79] B.G. Johnson, P.M. Gill, J.A. Pople, The performance of a family of density functional methods, J. Chem. Phys. 98 (1993) 5612–5626.
[80] M. Frisch, G. Trucks, H. Schlegel, G. Scuseria, M. Robb, J. Cheeseman, G. Scalmani, V. Barone, B. Mennucci, G. Petersson, 09, Revision D.01, Gaussian, Inc., Wallingford, CT, 2009.
[81] L.W. Chung, W. Sameera, R. Ramozzi, A.J. Page, M. Hatanaka, G.P. Petrova, T.V. Harris, X. Li, Z. Ke, F. Liu, The ONIOM method and its applications, Chem. Rev. 115 (2015) 5678–5796.
[82] M. Lundberg, Y. Sasakura, G. Zheng, K. Morokuma, Case studies of ONIOM (DFT: DFTB) and ONIOM (DFT: DFTB: MM) for enzymes and enzyme mimics, J. Chem. Theory Comput. 6 (2010) 1413–1427.
[83] J.W. Ochterski, Thermochemistry in Gaussian, Gaussian Inc., 2000, pp. 1–19.
[84] E. Jenwitheesuk, R. Samudrala, Improved prediction of HIV-1 protease-inhibitor binding energies by molecular dynamics simulations, BMC Struct. Biol. 3 (2003) 1.
[85] A.L. Perryman, J.H. Lin, J.A. McCammon, HIV-1 protease molecular dynamics of a wild-type and of the V82F/I84V mutant: possible contributions to drug resistance and a potential new target site for drugs, Protein Sci. 13 (2004) 1108–1123.
[86] D.I. Freedberg, R. Ishima, J. Jacob, Y.X. Wang, I. Kustanovich, J.M. Louis, D.A. Torchia, Rapid structural fluctuations of the free HIV protease flaps in solution: relationship to crystal structures and comparison with predictions of dynamics calculations, Protein Sci. 11 (2002) 221–232.
[87] U. Ryde, A fundamental view of enthalpy-entropy compensation, MedChemComm 5 (2014) 1324–1336.